

International Journal of Automation & Digital Transformation

Vol 2 Issue 1 (2023) 4 - 14

DOI: 10.54878/IJADT.574

Available at www.emiratesscholar.com



Modeling and Control of Electrical Model of PV Module

Bahij Zeina^a, Ismail Abdulla^b
Phd Student^a, Professor of Electrical Engineering^b
Rochester Institute of Technology - Dubai
zb6781@rit.edu (ESID 5830 9822 2022)

Abstract

The use of green energy has been of wide interest in recent decades. Photovoltaic systems are used to convert sunlight into electric energy. In this paper, an electrical model of the photovoltaic system is presented. Parameters from datasheet of a photovoltaic system, I(V) and P(V) characteristics plot are used to calculate the exact series and shunt resistances. Several experiments in smart energy lab of Rochester Institute of technology Dubai campus were performed to validate the PV electrical model. This model was controlled using converter with Maximum Power Point Tracking (MPPT) for a stabilized connection to a Microgrid.

Keywords:

Photovoltaic System, Solar Model, Voltage Open Circuit, Short Circuit Current, Maximum Power Point Tracking, Boost Converter.

I. INTRODUCTION

The performance of a solar cell can be demonstrated by measuring its current versus the voltage. The IV curve is the superposition of the IV curve of the solar cell diode in the dark with the light-generated current [1]. Both parameters, Voltage Open Circuit (VOC) and current short Circuit (ISC), define the IV curve. The power of a solar cell is defined as the voltage multiplied by the current at any point on the IV curve. With the IV curve, it is possible to determine the maximum power point (MPPT). Figure 1 shows the power versus the current (red line). The current and voltage where the maximum power point has two parameters that define the characteristics of the solar module. That power is the one delivered to the rest of the PV system and eventually to the load. Therefore, it is essential that the solar module operate at the maximum power. [2]

The simplest equivalent circuit of a solar cell is a current source connected in anti-parallel way with a light current source [3]. This model does not take into account the internal losses of the current. Figure 2 shows the equivalent circuit.

Using Kirchhoff law to calculate the output current:

$$I = I_{ph} - I_d \quad (1)$$

where I_{ph} is the photocurrent.

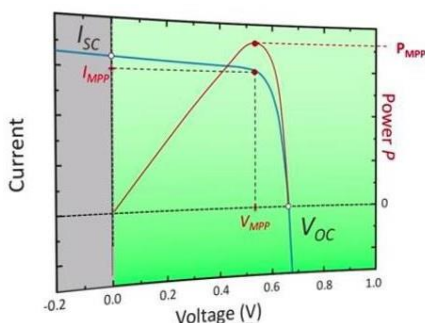
I_d is the diode current given by

$$I_d = I_0 \left[\exp\left(\frac{V}{N_s V_T}\right) - 1 \right] \quad (2)$$

where V is the voltage imposed on the diode.

V_T is the Thermal Voltage

$$V_T = k T_c / q \quad (3)$$



International Journal of Automation & Digital Transformation
Emirates Scholar
Figure 1 IV and PV characteristics of PV [2]

I_0 is the leakage current of the diode (A) T_c is the actual cell temperature (K).

k is the Boltzman constant (1.381×10^{-23} J/K) q is the electron charge (1.602×10^{-19} C)

N_s is the number of PV cells connected in series and A is the ideality factor depends on PV Technology

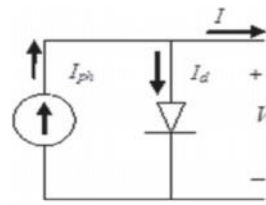


Figure 2 Simplest Equivalent Circuit of Solar Cell [3]

In real life, it is impossible to neglect current losses, so series resistance R_s and Parallel resistance R_p are added to the circuit. Series resistances are caused by the contact resistance between the metal contact and the silicon, the movement of current through the emitter and the base of the solar cell and the resistance of the top and rear metal contacts. While shunt resistance causes significant power losses typically due to manufacturing defects rather than poor solar cell design. Figure 3 shows the real circuit of a solar cell.

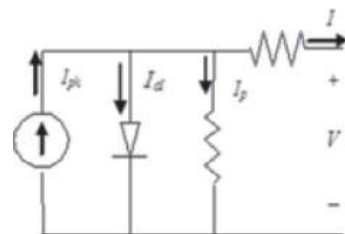


Figure 3 Real Life Equivalent Circuit of Solar Cell [3]

Adding series resistor will lead the revised I_d as:

$$I_d = I_0 \left[\exp\left(\frac{V + IR_s}{a}\right) - 1 \right] \quad (4)$$

where a is the thermal voltage given as

$$a = \frac{N_s A V_T}{q} \quad (5)$$

By applying Kirchhoff law to circuit in figure 2,

output current will be is the

$$I = I_{ph} - I_d - I_p \quad (6)$$

where I_p is the current across R_p The output current then is given as

$$I = I_{ph} - I_0 \left[\exp\left(\frac{V+IR_S}{a}\right) - 1 \right] - \frac{V+IR_S}{R_P} \quad (7)$$

$$\text{where } I_{ph} = \frac{G}{100} [I_{SCR} + K_I(T - 25)] \quad (8)$$

$$\text{and } I_0 = I_{or} \left(\frac{T}{T_r}\right)^3 \exp\left[\frac{qE_{G0}}{BK} \left(\frac{1}{T_r} - \frac{1}{T}\right)\right] \quad (9)$$

where I_{sc} is the short circuit current.

$$I_{ph} = \frac{G}{G_{ref}} (I_{ph,ref} + \mu_{sc}\Delta T) \quad (14)$$

where G is the Irradiance (W/m^2)

G_{ref} is the Irradiance at $STC = 1000 W/m^2$

$$\Delta T = T_c - T_{c,ref} \text{ (Kelvin)} \quad (15)$$

$T_{c,ref}$ is the Cell temperature at $STC = 25 + 273 = 298 K$,

μ_{sc} is the Coefficient temperature of short circuit current (A/K), provided by the manufacturer

$I_{ph,ref}$ is the Photocurrent (A) at STC .

At the end of that study $R_s = 0.45 \Omega$ and $R_p = 310.0248 \Omega$.

II. LITERATURE REVIEW

In order to find the PV best model, several parameters have to be calculated. In [4], a model of moderate complexity was used where the temperature dependence of the photo-current I_L , saturation current of the diode I_0 , series resistance R_S were included, but effect of the shunt resistance was neglected.

The equations to describe the IV characteristics where as follows:

$$\text{Photo current: } I_L = G \frac{I_{SC}(T_1)}{G_0} [1 + K_0(T - T_1)] \quad (10)$$

$$\text{Where } K_0 = \frac{I_{SC}(T_2) - I_{SC}(T_1)}{T_2 - T_1} \quad (11)$$

$$I_0 = I_{d0} \left(\frac{T}{T_r}\right)^{3/n} \exp\left[-\frac{q}{nK} V_g \left(\frac{1}{T_r} - \frac{1}{T}\right)\right] \quad (12)$$

$$I_{d0} = \frac{I_{SC}(T_1)}{\exp\left(\frac{qV_{OC}(T_1)}{T_1} - 1\right)} \quad (13)$$

In [5] I_{ph} , I_0 , R_S , R_P were calculated. Photocurrent is calculated assuming that when PV model is short-circuited, $I_{ph} = I_{SCref}$, which is the short circuit current reference, calculated at the standard test conditions (STC), the photocurrent

III. MODELING OF PV

The physical model of the PV cell under study is a polycrystalline solar model found in Smart Energy lab at RIT- Dubai. Specifications of this model are present in

Table 1. Table 1 Parameters of PV at STC

Parameters	Values
Maximum Power Point P_{mp} (W)	4.56
Maximum Current Point I_{mp} (A)	0.24
Maximum Voltage Point V_{mp} (V)	19
Short Circuit Current I_{sc} (A)	0.26
Open Circuit Voltage V_{oc}	22 V
N_{oct} ($^{\circ}C$)	45
Coefficient temperature μ_{sc} (K^0)	1.3×10
K_d	-72.5×10

A. VALIDATION OF VOLTAGE OPEN CIRCUIT

model are present in V_{OC} is calculated experimentally to validate the physical model. V_{oc} is the maximum voltage that a PV system can produce. It occurs at zero current. (Fig.1)

V_{OC} changes with changing temperature, irradiance and angle of incidence. [6-7]. An experiment was conducted

in the lab to measure the VOC:

The solar module has a lamp that can emit light with different intensities (irradiances). Also, the azimuth and elevation angles of the lamp can vary so that it can present different positions of the sunlight to enable studies of the solar panel power during a day where sun position varies. The analog/digital multimeter shown is used to measure the voltage and current. The solar module and digital multimeter are connected together as shown in Figure 4.



Figure 4 Connecting the Solar Module to the Multimeter to Measure the Voltage

The halogen lamp is positioned perpendicularly over the solar module. The voltage was measured at different irradiances. VOC is the maximum voltage reached at maximum irradiance.

B. VALIDATION OF SHORT CIRCUIT CURRENT

The short-circuit current is the largest possible current a PV cell can supply. It is measured when the voltage of the PV cell is zero using an ammeter with a very low internal resistance connected directly to the PV cell's terminals.

Same equipment were used for measuring the short circuit current and the open circuit voltage, but connection with the multimeter differs. Here, the positive terminal of the solar module was connected to the I pin of the multimeter as shown in Figure 5. Irradiance was increased and current was recorded when the halogen lamp is positioned perpendicularly over the solar module.

International Journal of Automation & Digital Transformation

Emirates Scholar



Figure 1 Connection of the Solar Module with the Multimeter to Measure the Current

C. RECORDING IV CHARACTERISTICS

IV characteristics at variable irradiance of the solar module was plotted in the smart energy lab. The sun and panel angles were set to 0° . The elevation angle was set to 90° so that the halogen lamp is positioned perpendicularly over the solar module. The solar module was connected to the multimeter as shown in Figure 6. Irradiance of the solar module was set to its maximum value: 380 W/m^2 . The circuit was short circuited. (Potentiometer was set to 0Ω). Potentiometer were slowly moved to its maximum value, at that time current and voltage were recorded.



Figure 6 Connection of the Solar Module with the Multimeter to Measure the Current

D. CALCULATING SERIES AND SHUNT RESISTANCES

Parameters V_{oc} , I_{sc} , V_{mp} and I_{mp} were used to calculate series and shunt resistances. These resistances were not mentioned in Table 1. First, equations of photocurrent and the saturation current of the diode are taken from [5], which does not consider shunt resistance, were used to plot the IV and PV characteristics. Then, series resistance will be incremented from 0 till the maximum power point is achieved at the maximum voltage at STC referring to Table 1. Shunt resistance is then calculated using equation (17).

Taking the most remarkable points at standard test condition: the voltage at open circuit ($I = 0$, $V = V_{oc,ref}$), the current at short circuit ($V = 0$, $I = I_{sc,ref}$), and the voltage ($V_{mp,ref}$) and current ($I_{mp,ref}$) at maximum power, the reverse saturation current is:

$$I_0 = I_{sc,ref} \exp\left(\frac{V_{oc,ref}}{a} \left(\frac{T_c}{T_{c,ref}}\right)^3 \exp\left[\left(\frac{qE_G}{AK}\right) \left(\frac{1}{T_{c,ref}} - \frac{1}{T_c}\right)\right]\right)$$

The series and shunt resistors are calculated at maximum power point, R_s is first set to zero and then slowly increased until experimental and theoretical MPP are equal, then R_p is calculated using the following relationship:

$$R_p = \frac{V_{mp,ref} + I_{mp,ref} R_s}{I_{sc,ref} - I_{sc,ref} \left\{ \exp\left[\frac{V_{mp,ref} + I_{mp,ref} R_s - V_{oc,ref}}{a}\right] + I_{sc,ref} \left\{ \exp\left(-\frac{V_{oc,ref}}{a}\right) - \frac{P_{max}}{V_{mp,ref}} \right\} \right\}} \quad (17)$$

Converters are widely used to control the power flow, voltage, system balancing, maximum power point tracking and fault protection. [8] Converters switched mode power supplies, which can convert the DC voltage from one level to another.

International Journal of Automation & Digital Transformation
It can step up or step down the dc voltage.
Emirates Scholar source. Stepping up the voltage means stepping

down the current and vice versa.

The dc-dc converters are widely used for traction motor control in electronic automobiles, trolley cars, marine hoists, forklift trucks, and mine haulers. They provide smooth acceleration control, high efficiency, and fast dynamic response. DC-DC converters can be used in regenerative braking of dc motors to return energy back into the supply, than this feature results in energy savings for transportation systems with frequent stops. [14] DC converters are used in dc voltage regulators and also are used in conjunction with an inductor, to generate a dc current source, especially for the current source inverter.

A. CONTROL OF PV MODEL

PV module produces variable power depending on irradiance and temperature and it reaches maximum power point, product of V_{mpp} and I_{mpp} , at specific irradiance and temperature. Maximum Power Point Tracking (MPPT) algorithm is used to extract maximum power from renewable energy resources like wind turbines and PV, under all conditions, since they produce variable power due to their intermittency nature [9-10]. Its main objective is to find the maximum power point and keep the load resistance, characterized by the I-V curve, at that point. MPPT devices are integrated into an electric power converter system that provides current or voltage conversion, regulation for driving various loads.

Many researchers has proposed different strategies to extract maximum power form PV using MPPT algorithm. In [11] tracking maximum power point using linear relationship between maximum voltage and open circuit voltage. In [12] the author used a look-up table to track techniques with measurement and comparison. The use of microcontrollers in power systems enables the implementation of AI techniques. In [13] Artificial Neural Network (ANN) MPPT controller was proposed based on fixed and variable step size, is proposed. In this work, a number of layers and neurons, parameters of training algorithm of the MPPT Controller were generated and then used in PV system.

Perception and Observation (P&O) technique is widely used. Its main advantage is that it is independent of PV generator characteristics, like

solar intensity and cell temperature and can be

implemented in analogue and digital circuits. It perturbs the operating point to let the voltage fluctuate around the maximum power point voltage despite the variation of irradiance and temperature[14]. This strategy is widely used because of its simplicity and efficiency. However, it lacks fast adaptability which is important to track fast transients under varying environment conditions[15-17]. In this paper, incremental conductance MPPT is used. The IncCond method is the one which overrides over the aforementioned drawbacks. In this method, the array terminal voltage is always adjusted according to the MPP voltage. It is based on the incremental and instantaneous conductance of the PV module [17-22].

A boost converter of 5 kHz and 300 V reference is used to control the output of PV system, this boost converter is controlled by MPPT (incremental conductance + integral regulator).

Figure 7 shows the MPPT used for control of boost converter. Output voltage and current of the PV system are the inputs to the MPPT subsystem. Deblock is used to switch MPPT on or off. MPPT subsystem is shown in Figure 6. Output of the MPPT is the DC voltage reference subtracted from the Duty cycle and then used to generate pulses of the Pulse Width Modulation of frequency 5 kHz and initial value of 0.25. DC-DC converter is shown in Figure 7.

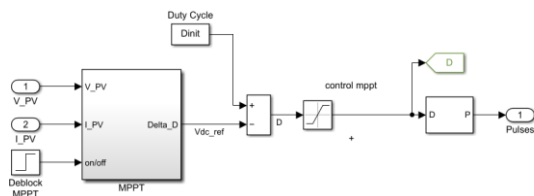


Figure 7 MPPT Boost Converter Control

Figure 8 shows the incremental conductance MPPT subsystem used. Its inputs are the output voltage and current of the PV system. The array terminal voltage is always adjusted according to the MPP voltage. It is based on the incremental and instantaneous conductance of the PV module.

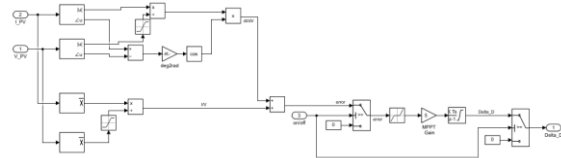


Figure 8 MPPT subsystem

Boost converter (Figure 9) boost the output voltage of the PV system to 300 V. When the switch is closed the inductor store energy and there is no current delivered the diode, energy will be supplied by the capacitor charge. Energy stored in the inductor will be delivered to the load to boost output voltage and recharge the capacitor when the switch is open. Inductor immediately reverse its electromagnetic field to opposes any drop in current. Voltage is controlled by varying the duty cycle that is pulses generated from the MPPT subsystem.

$$V_o = \frac{V_s}{1-D} \quad (18)$$

Capacitor of capacitance 100 μF is used as a DC link. Resistor of resistance 0.005 Ω and inductor of inductance 5 mH was used.

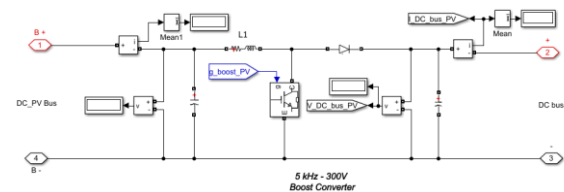


Figure 9 Boost Converter used to control PV system.

V. RESULT

A. VALIDATION OF VOLTAGE OPEN CIRCUIT

Figure 10 shows recorded voltage for different irradiances. It is clear that after certain irradiance (100 W/m²) the voltage is nearly constant. The rapid variation in voltage is shown at irradiances below 100 W/m². So open-circuit voltage is not a linear function of the irradiance. The open circuit voltage can be calculated at the maximum irradiance from the PV module, which is 21 V.

Table 1 shows that the open circuit voltage is 21.8 V which is approximately the same as the measured value.

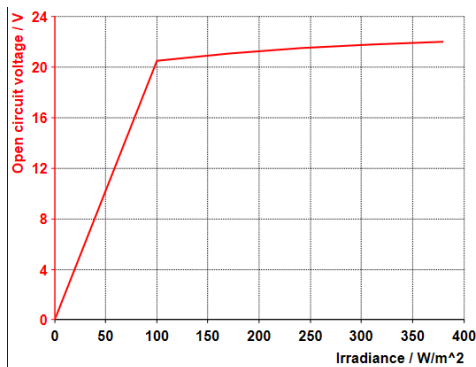


Figure 10 Voltages as a function of Irradiances

B. VALIDATION OF SHORT CIRCUIT CURRENT

Figure 11 shows recorded current for different irradiances. It is clear that the current is linearly dependent on the irradiance. The short circuit current of this solar module, which is the maximum current generated from the solar module, is 210 mA. The maximum irradiance for the solar module used is 380 W/m². In our model, the maximum irradiance is 1000 W/m². Due to the fact that, the current is linearly dependent on the voltage we can calculate the current at the maximum irradiance of 1000 W/m².

Line equation that describes the relation between current and irradiance is given as follows:

$$Y=0.5 x \text{ for } x<240 \quad (19)$$

$$Y= 0.7142x \text{ for } x>240 \quad (20)$$

Therefore, the current at 1000 W/m² is 150 mA which is much less than the theoretical calculation shown in Table 1.

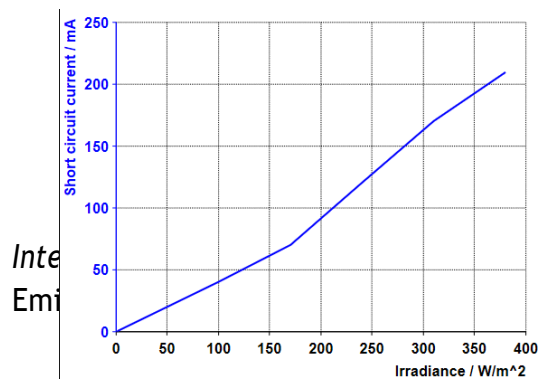


Figure 11 Current as a function of Irradiances

Same experiment was done after few minutes. A big change in the current values was noticed as shown in Figure 12.

A new equation that describes the relation between the current and irradiance is obtained from the new measured values.

$$Y= x \text{ for } x<100 \quad (21)$$

$$Y= 1.142x \text{ for } x>100 \quad (22)$$

Then, the current at 1000 W/m² is 480 mA which is much less than the theoretical calculation shown in Table 1. The experimental short circuit current measurement was not accurate since it is highly dependent on irradiance and temperature, so its value will change at different times as the temperature of the solar module will change by time as long as the lamp is on that causes an increase in its temperature. The theoretical value of the short circuit current which is 3.11 mA was considered in this study.

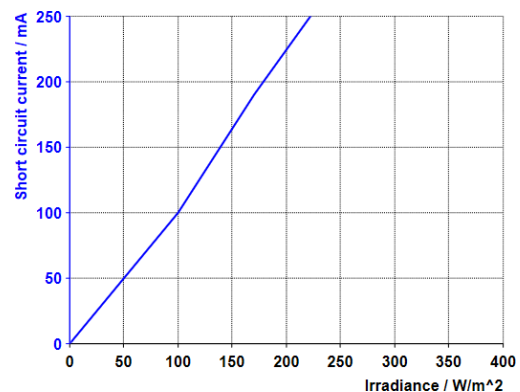


Figure 12 Current as a function of Irradiances after Few Minutes.

C. RECORDING IV CHARACTERISTICS

Figure 13 shows the IV characteristics of the Solar Module. Open Circuit voltage is the intersection of the curve with the x-axis when the net current is zero. It is the same as the experimental value measured in the first experiment "Measurement of the Open Circuit Voltage" which is 21.8 V. However, the short circuit current is 250 mA which differs from the theoretical value (0.311 A) since the maximum irradiance in the

theory part is 1000 W/m² and the maximum irradiance

Figure 14 IV characteristics without Rp

of the solar module is 380 W/m². Also, as discussed in the second experiment the current is highly dependent on the temperature, so the more the lamp is on, the more the solar module is exposed to the light and the higher temperature will produce higher current. This experiment was done after the measurement of the first values when the short circuit current was 210 mA and before the measurement of the second values when the short circuit current was 420 mA. This verifies that the longer time the solar module is exposed to light the higher values of current will be produced.



Figure 13 IV characteristics of the Solar Module

D. CALCULATING SERIES AND SHUNT OF THE SOLAR MODULE

Figure 14 shows the IV characteristics in Rs model without considering shunt resistance. As series resistance increases, maximum voltage point decreases and approaches the maximum power point (17V). When Rs= 0.9 Ω, curve showed MPP maximum voltage point.

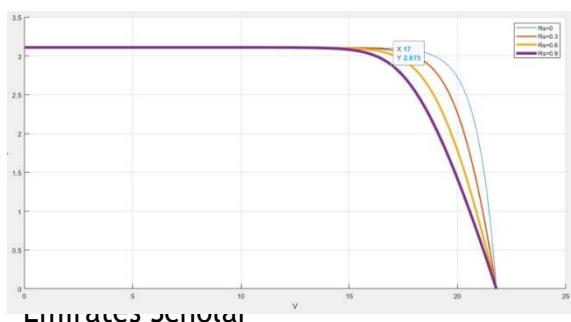


Figure 15 shows the PV characteristics in Rs model without considering shunt resistance. As series resistance increases, maximum power point decreases and approaches the maximum power point (49 W). When Rs= 0.9 Ω, curve showed MPP maximum power at 49W. Rp was found to be 185 Ω after substituting Rs in (17).

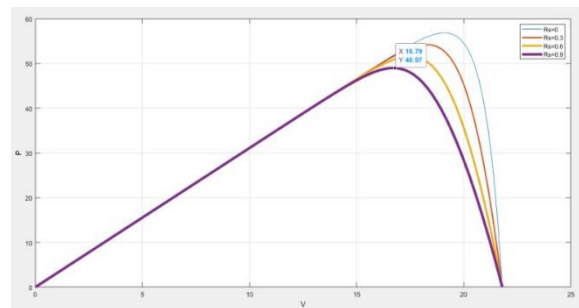


Figure 15 PV characteristics without Rp

Figure 16 represents IV characteristics for the PV model using series and parallel resistances at STC. MPP and maximum current were achieved at 17 V and that verified our model. Imp was 2.85 at 17.004 V (Accurate voltage and current at 17 V could not be measured due to the step size of the cursor in Matlab).

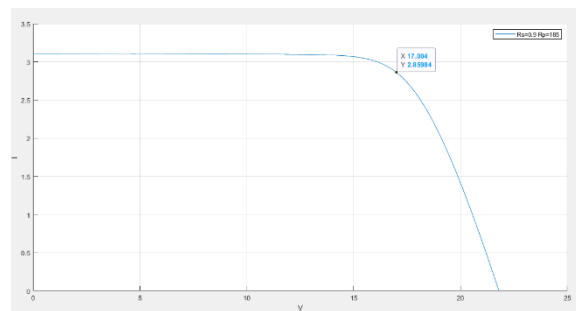


Figure 16 IV characteristics with series and parallel resistances

Figure 17 represents PV characteristics for the PV model using series and parallel resistances at STC. MPP and maximum current were achieved at 17 V and that verified our model. Pmp was 48.774 A at 16.7 V. (Accurate power and current at 17 V could not be measured due to the step size of the cursor in Matlab).

Figure 19 PV Output Voltage

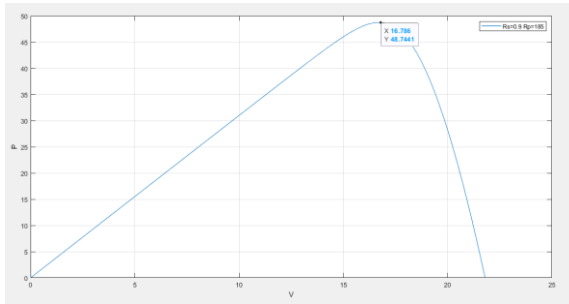


Figure 7 PV characteristics with series and parallel resistances

E. PV DAILY OUTPUT

Figure 18 shows the output current of the PV system before control. Current changes proportionally with changing irradiance. When irradiance is zero, no output current from PV is generated. When irradiance started increasing gradually, this current increases to reach a maximum value of 120 A.

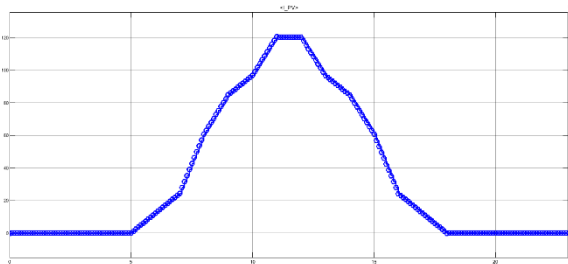
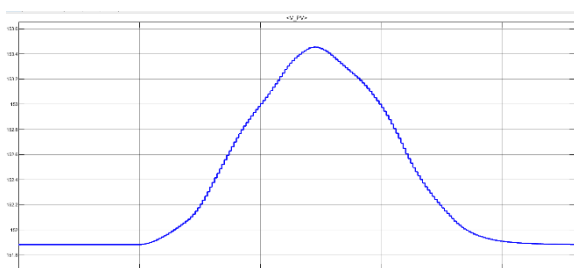


Figure 18 PV Output Current

Figure 19 shows the output voltage of the PV system before control. The voltage is about 151 V when irradiance is zero. At maximum irradiance, the voltage reaches 153.45 V. Irradiance effect on this voltage is weak compared to the effect on the current. This verified the PV model discussed in chapter 3. We have 10 series connected panels and each one has the output voltage at maximum power point of 17 V.



F. RESULT OF THE PV MODEL CONTROL SYSTEM

Figure 20 shows the output voltage of the PV system, where the output voltage at the DC bus increases to reach 437 V. Then it decreases to a constant value, for the rest of the day, at 300 V, which is the DC bus voltage required.

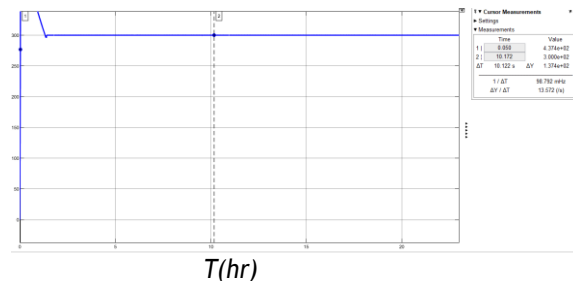


Figure 20 DC Bus of the PV system

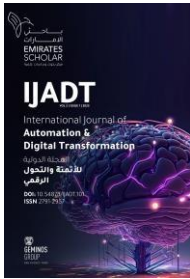
VI. CONCLUSION

The presented work calculated the exact series and shunt resistance of a PV model. Maximum Power Point (MPPT) parameters (current, voltage and power) have been taken from the datasheet and I(V) and P(V) characteristics curves were plotted at different resistances until MPP was reached. Then, the PV system relationship between series and shunt resistances were used to calculate the shunt resistance.

It is important to compute R_s , even if it is given by a manufacturer because the experimental Maximum Power Point does not match with the computed one. Only one pair satisfies the condition of matching the modeled and the experimental peak power. So, R_s is iteratively increased until satisfying the condition. The proposed R_p model gave ($R_s = 0.9 \Omega$, $R_p = 185 \Omega$).

A boost converter was used to control PV system. This boost converter was controlled with MPPT (incremental conductance) used for control. Output of the MPPT is the DC voltage reference subtracted from the Duty cycle and then used to generate pulses of the Pulse Width Modulation.

The output voltage at the DC bus increases to reach 437 V, then it decreases to a constant value, for the rest of the day, of 300 V which is the DC bus voltage required.



VII. REFERENCE

WALKER, G. Evaluating MPPT Converter Topologies using a Matlab PV Model. University of Queensland. Australia.

S. Ma Lu “Modelling, Control and Simulation of a Microgrid based on PV System, Battery System and VSC” January 2018.

H. Bellia a,*, R. Youcef b, M. Fatima b”A detailed modeling of photovoltaic module using MATLAB” National Research Institute of Astronomy and Geophysics NRIAG Journal of Astronomy and Geophysics April 2014

F. Mohammed “MICROGRID MODELLING AND SIMULATION” Espoo March 2016

F. Mohammed “MICROGRID MODELLING AND SIMULATION” Espoo March 2016

Hua, C., Lin, J.: ‘An on-line MPPT algorithm for rapidly changing illuminations of solar arrays’, *Renew. Energy*, 2003, **28**, (7), pp. 1129-1142

Malik, A.Q., Chee, L., Sheng, T.K., *et al.*: ‘Influence of temperature on the performance of photovoltaic polycrystalline silicon module in the Bruneian climate’, *ASEAN J. Sci. Technol. Dev.*, 2010, **26**, (2), pp. 61-72

Muhammad H. Rashid, “Power Electronics: Circuits, Devices, and Application”. THIRD EDITION
Design and simulation of dc Microgrid in belize D. W. Hart, Power electronics. Tata McGraw-Hill Education, 2011.

Masoum, M.A.S.; Dehbonei, H.; Fuchs, E.F. Theoretical and experimental analyses of photovoltaic systems with voltage and current based maximum power-point tracking. *IEEE Trans. Energy Convers.* **2002**,

17, 514-522.

Ram, J.P., Babu, T.S., Rajasekar, N.: ‘A comprehensive review on solar PV maximum power point tracking techniques’, *Renew. Sustain. Energy Rev.*, 2017, **67**, pp. 826-847
Kumar, D., Chatterjee, K.: ‘A review of conventional and advanced MPPT algorithms

for wind energy systems’, *Renew. Sustain. Energy Rev.*, 2016, **55**, pp. 957-970

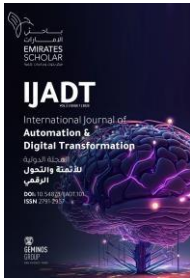
Yamashita, H.; Tamahashi, K.; Michihira, M.; Tsuyoshi, A.; Amako, K.; Park, M. A novel simulation technique of the PV generation system using real weather conditions. In *Proceedings of the Power Conversion Conference, Osaka, Japan, 2-5 April 2002*; Volume 2, pp. 839-844.

Messalti, S.; Harrag, A.; Loukriz, A. A new variable step size neural networks {MPPT} controller: Review, simulation and hardware implementation. *Renew. Sustain. Energy Rev.* 2017, **68**, 221- 233.

M. A. Elgendy, B. Zahawi, and D. J. Atkinson, “Assessment of perturb and observe MPPT algorithm implementation techniques for PV pumping applications,” *IEEE Transactions on Sustainable Energy*, vol. 3, no. 1, pp. 21-33, 2012.

H. Malek and Y. Chen, “BICO MPPT: a faster maximum power point tracker and its application for photovoltaic panels
Osakada, –Maximum photovoltaic power tracking: An algorithm for rapidly changing atmospheric conditions, *Proc. Inst. Elect. Eng.—Gener, Transmits. Distrib.*, vol. 142, no. 1, pp. 59-64, Jan. 1995. ,” *International Journal of Photoenergy*, vol. 2014, Article ID 586503, 9 pages, 2014.

Dabra, V., Paliwal, K. K., Sharma, P., & Kumar, N. (2017). Optimization of photovoltaic power system: A comparative study. *Proceeding and Control of Modern Power Systems*, 2(1), 3.



F. Liu, S. Duan, F. Liu, B. Liu, and Y. Kang, –A variable step size INC MPPT method for PV systems, II IEEE Trans. Ind. Electron., vol. 55, no. 7, pp. 2622-2628, Jul. 2008

K. H. Hussein, I. Muta, T. Hoshino, and M. B. Liu, S. Duan, F. Liu, and P. Xu, –Analysis and improvement of maximum power point tracking algorithm based on incremental conductance method for photovoltaic array, II in Proc. IEEE PEDS, 2007, pp. 637-641.

Y.-C. Kuo, T.-J. Liang and J.-F. Chen, –Novel maximum power-point tracking controller for photovoltaic energy conversion system, II IEEE Trans. Ind. Electron, vol. 48, no. 3, pp. 594-601, Jun. 2001.